Charm counting in b decays

D. Buskulic, I. de Bonis, D. Decamp, P. Ghez, C. Goy, J.P. Lees, A. Lucotte,
M.N. Minard, J.Y. Nief, P. Odier, et al.

Charm counting in b decays

The ALEPH collaboration

Abstract

The inclusive production of charmed particles in $Z \rightarrow b\bar{b}$ decays has been measured from the yield of D^0, D^+, D_s^+ and Λ_c^+ decays in a sample of $q\bar{q}$ events with high b purity collected with the ALEPH detector from 1992 to 1995.

From these measurements, adding the charmonia production rate and an estimate of the charmed strange baryon contribution, the average number of charm quarks per b decay is determined to be $n_c = 1.230 \pm 0.036 \pm 0.038 \pm 0.053$, where the uncertainties are due to statistics, systematic effects and branching ratios, respectively.

(To be submitted to Physics Letters B)

---

*See the following pages for the list of authors.

The ALEPH Collaboration

D. Buskulic, I. De Bonis, D. Decamp, P. Ghez, C. Goy, J.-P. Lees, A. Lucotte, M.-N. Minard, J.-Y. Nief, P. Odier, B. Pietrzyk

Laboratoire de Physique des Particules (LAPP), IN[2]P[3]-CNRS, 74019 Annecy-le-Vieux Cedex, France

M.P. Casado, M. Chmeissani, J.M. Crespo, M. Delfino, I. Efthymiopoulos,[1] E. Fernandez, M. Fernandez-Bosman, Ll. Garrido,[15] A. Juste, M. Martinez, S. Orteu, C. Padilla, I.C. Park, A. Pascual, J.A. Perlas, I. Riu, F. Sanchez, F. Teubert

Institut de Fisica d'Altes Energies, Universitat Autonoma de Barcelona, 08193 Bellaterra (Barcelona), Spain[7]

A. Colaleo, D. Creanza, M. de Palma, G. Gelao, M. Girone, G. Iaselli, G. Maggi, M. Maggi, N. Marinelli, S. Nuzzo, A. Ranieri, G. Raso, F. Ruggieri, G. Selvaggi, L. Silvestris, P. Tempesta, A. Tricomi,[3] G. Zito

Dipartimento di Fisica, INFN Sezione di Bari, 70126 Bari, Italy

X. Huang, J. Lin, Q. Ouyang, T. Wang, Y. Xie, R. Xu, S. Xue, J. Zhang, L. Zhang, W. Zhao

Institute of High-Energy Physics, Academia Sinica, Beijing, The People's Republic of China[8]

R. Alemany, A.O. Bazarko, G. Bonvicini,[23] P. Bright-Thomas, M. Cattaneo, F. Cerutti, P. Comas, P. Coyle, H. Drevermann, R.W. Forty, M. Frank, R. Hagelberg, J. Harvey, P. Janot, B. Jost, E. Kneringer, J. Knobloch, I. Lehraus, G. Lutters, E.B. Martin, P. Mato, A. Minten, R. Miquel, Ll.M. Mir,[2] L. Moneta, T. Oest,[20] A. Pacheco, J.-F. Pusztaszeri, F. Ranjard, P. Rensing,[12] G. Rizzo, L. Rolandi, D. Schlatter, M. Schmelling,[24] M. Schmitt, O. Schneider, W. Tejessy, I.R. Tomalin, A. Venturi, H. Wachsmuth, A. Wagner

European Laboratory for Particle Physics (CERN), 1211 Geneva 23, Switzerland

Z. Ajaltouni, A. Barrès, C. Boyer, A. Falvard, P. Gay, C. Guicheney, P. Henrard, J. Jousset, B. Michel, S. Monteil, J-C. Montret, D. Pallin, P. Perret, F. Podlyski, J. Proriol, P. Rosnet, J.-M. Rossignol

Laboratoire de Physique Corpusculaire, Université Blaise Pascal, IN[2]P[3]-CNRS, Clermont-Ferrand, 63177 Aubière, France

T. Fearnley, J.B. Hansen, J.D. Hansen, J.R. Hansen, P.H. Hansen, B.S. Nilsson, B. Rensch, A. Wäänänen

Niels Bohr Institute, 2100 Copenhagen, Denmark[9]

A. Kyriakis, C. Markou, E. Simopoulou, I. Siotis, A. Vayaki, K. Zachariadou

Nuclear Research Center Demokritos (NRCD), Athens, Greece

A. Blondel, G. Bonneaud, J.C. Brient, P. Bourdon, A. Rougé, M. Rumpf, A. Valassi,[6] M. Verderi, H. Videau[21]

Laboratoire de Physique Nucléaire et des Hautes Energies, Ecole Polytechnique, IN[2]P[3]-CNRS, 91128 Palaiseau Cedex, France

D.J. Candlin, M.I. Parsons

Department of Physics, University of Edinburgh, Edinburgh EH9 3JZ, United Kingdom[10]

E. Focardi,[21] G. Parrini

Dipartimento di Fisica, Università di Firenze, INFN Sezione di Firenze, 50125 Firenze, Italy

M. Corden, C. Georgiopoulos, D.E. Jaffe

Supercomputer Computations Research Institute, Florida State University, Tallahassee, FL 32306-4052, USA [13,14]

A. Antonelli, G. Bencivenni, G. Bologna,[4] F. Bossi, P. Campana, G. Capon, D. Casper, V. Chiarella, G. Felici, P. Laurelli, G. Mannocchi,[5] F. Murtas, G.P. Murtas, L. Passalacqua, M. Pepe-Altarelli

Laboratori Nazionali dell'INFN (LNF-INFN), 00044 Frascati, Italy

L. Curtis, S.J. Dorris, A.W. Halley, I.G. Knowles, J.G. Lynch, V. O'Shea, C. Raine, P. Reeves, J.M. Scarr, K. Smith, P. Teixeira-Dias, A.S. Thompson, F. Thomson, S. Thorn, R.M. Turnbull

Department of Physics and Astronomy, University of Glasgow, Glasgow G12 8QQ, United Kingdom[10]

U. Becker, C. Geweniger, G. Graefe, P. Hanke, G. Hansper, V. Hepp, E.E. Kluge, A. Putzer, M. Schmidt, J. Sommer, H. Stenzel, K. Tittel, S. Werner, M. Wunsch

Institut für Hochenergiephysik, Universität Heidelberg, 69120 Heidelberg, Fed. Rep. of Germany[16]

D. Abbaneo, R. Beuselinck, D.M. Binnie, W. Cameron, P.J. Dornan, A. Moutoussi, J. Nash, J.K. Sedgbeer, A.M. Stacey, M.D. Williams

Department of Physics, Imperial College, London SW7 2BZ, United Kingdom[10]

G. Dissertori, P. Girtler, D. Kuhn, G. Rudolph

Institut für Experimentalphysik, Universität Innsbruck, 6020 Innsbruck, Austria[18]

A.P. Betteridge, C.K. Bowdery, P. Colrain, G. Crawford, A.J. Finch, F. Foster, G. Hughes, T. Sloan, M.I. Williams

Department of Physics, University of Lancaster, Lancaster LA1 4YB, United Kingdom[10]

A. Galla, I. Giehl, A.M. Greene, C. Hoffmann, K. Jakobs, K. Kleinknecht, G. Quast, B. Renk, E. Rohne, H.-G. Sander, P. van Gemmeren, C. Zeitnitz

Institut für Physik, Universität Mainz, 55099 Mainz, Fed. Rep. of Germany[16]

J.J. Aubert,[21] A.M. Bencheikh, C. Benchouk, A. Bonissent, G. Bujosa, D. Calvet, J. Carr, C. Diaconu, F. Etienne, N. Konstantinidis, P. Payre, D. Rousseau, M. Talby, A. Sadouki, M. Thulasidas, K. Trabelsi

Centre de Physique des Particules, Faculté des Sciences de Luminy, IN^{2}P^3-CNRS, 13288 Marseille, France

M. Aleppo, F. Ragusa[21]

Dipartimento di Fisica, Università di Milano e INFN Sezione di Milano, 20133 Milano, Italy

C. Bauer, R. Berlich, W. Blum, V. Büscher, H. Dietl, F. Dydak,[21] G. Ganis, C. Gotzhein, H. Kroha, G. Lütjens, G. Lutz, W. Männer, H.-G. Moser, R. Richter, A. Rosado-Schlosser, S. Schael, R. Settles, H. Seywerd, R. St. Denis, H. Stenzel, W. Wiedenmann, G. Wolf

Max-Planck-Institut für Physik, Werner-Heisenberg-Institut, 80805 München, Fed. Rep. of Germany[16]

J. Boucrot, O. Callot, Y. Choi,[26] A. Cordier, M. Davier, L. Duflot, J.-F. Grivaz, Ph. Heusse, A. Höcker, A. Jacholkowska, M. Jacquet, D.W. Kim,[19] F. Le Diberder, J. Lefrançois, A.-M. Lutz, I. Nikolic, H.J. Park,[19] M.-H. Schune, S. Simion, J.-J. Veillet, I. Videau, D. Zerwas

Laboratoire de l'Accélérateur Linéaire, Université de Paris-Sud, IN^{2}P^3-CNRS, 91405 Orsay Cedex, France

P. Azzurri, G. Bagliesi, G. Batignani, S. Bettarini, C. Bozzi, G. Calderini, M. Carpinelli, M.A. Ciocci, V. Ciulli, R. Dell'Orso, R. Fantechi, I. Ferrante, L. Foà,[1] F. Forti, A. Giassi, M.A. Giorgi, A. Gregorio, F. Ligabue, A. Lusiani, P.S. Marrocchesi, A. Messineo, F. Palla, G. Sanguinetti, A. Sciabà, P. Spagnolo, J. Steinberger, R. Tenchini, G. Tonelli,[25] C. Vannini, P.G. Verdini

Dipartimento di Fisica dell'Università, INFN Sezione di Pisa, e Scuola Normale Superiore, 56010 Pisa, Italy

G.A. Blair, L.M. Bryant, J.T. Chambers, Y. Gao, M.G. Green, T. Medcalf, P. Perrodo, J.A. Strong, J.H. von Wimmersperg-Toeller

Department of Physics, Royal Holloway & Bedford New College, University of London, Surrey TW20 OEX, United Kingdom[10]

D.R. Botterill, R.W. Clifft, T.R. Edgecock, S. Haywood, P. Maley, P.R. Norton, J.C. Thompson, A.E. Wright

Particle Physics Dept., Rutherford Appleton Laboratory, Chilton, Didcot, Oxon OX11 OQX, United Kingdom[10]

B. Bloch-Devaux, P. Colas, S. Emery, W. Kozanecki, E. Lançon, M.C. Lemaire, E. Locci, P. Perez,

J. Rander, J.-F. Renardy, A. Roussarie, J.-P. Schuller, J. Schwindling, A. Trabelsi, B. Vallage

CEA, DAPNIA/Service de Physique des Particules, CE-Saclay, 91191 Gif-sur-Yvette Cedex, France[17]

S.N. Black, J.H. Dann, R.P. Johnson, H.Y. Kim, A.M. Litke, M.A. McNeil, G. Taylor

Institute for Particle Physics, University of California at Santa Cruz, Santa Cruz, CA 95064, USA[22]

C.N. Booth, R. Boswell, C.A.J. Brew, S. Cartwright, F. Combley, A. Koksal, M. Letho, W.M. Newton, J. Reeve, L.F. Thompson

Department of Physics, University of Sheffield, Sheffield S3 7RH, United Kingdom[10]

A. Böhrer, S. Brandt, G. Cowan, C. Grupen, J. Minguet-Rodriguez, F. Rivera, P. Saraiva, L. Smolik, F. Stephan,

Fachbereich Physik, Universität Siegen, 57068 Siegen, Fed. Rep. of Germany[16]

M. Apollonio, L. Bosisio, R. Della Marina, G. Giannini, B. Gobbo, G. Musolino

Dipartimento di Fisica, Università di Trieste e INFN Sezione di Trieste, 34127 Trieste, Italy

J. Rothberg, S. Wasserbaech

Experimental Elementary Particle Physics, University of Washington, WA 98195 Seattle, U.S.A.

S.R. Armstrong, P. Elmer, Z. Feng,[27] D.P.S. Ferguson, Y.S. Gao,[28] S. González, J. Grahl, T.C. Greening, O.J. Hayes, H. Hu, P.A. McNamara III, J.M. Nachtman, W. Orejudos, Y.B. Pan, Y. Saadi, I.J. Scott, A.M. Walsh,[29] J. Walsh, Sau Lan Wu, X. Wu, J.M. Yamartino, M. Zheng, G. Zobernig

Department of Physics, University of Wisconsin, Madison, WI 53706, USA[11]

1   Introduction

The discrepancy between the experimental value of $BR(b \to \ell\nu X)$ and its theoretical prediction [1, 2] is a long standing problem in b physics. The measurement of the average number of charm quarks per b decay, n_c, is relevant for the understanding of this discrepancy. The theoretical predictions of these two quantities are correlated and therefore comparisons between experimental measurements and theory in the plane n_c vs $BR(b \to \ell\nu X)$ are more powerful than for the individual quantities alone.

Recent theoretical papers on this subject [3, 4], based on a model-independent study of spectator effects and on the calculation of the next-to-leading order radiative corrections to the decay $b \to c\bar{c}s$, give precise estimates of n_c and $BR(B \to \ell\nu X)$. In [4] values of $n_c = 1.21 \pm 0.06$ and $BR(B \to \ell\nu X) = (12.0 \mp 1.0)\%$ are predicted for the on-shell renormalization scheme and a renormalization scale $\mu = m_b$. If the renormalization scale μ is moved to $m_b/2$ the predicted values are $n_c = 1.22 \pm 0.06$ and $BR(B \to \ell\nu X) = (10.9 \mp 1.0)\%$. The errors are anticorrelated and are mainly due to the uncertainty on the input quark mass ratio m_c/m_b, which is varied in the range 0.25-0.33.

These theoretical predictions refer to B mesons; they must be corrected [5] to be compared with the LEP results, where a different b hadron composition is produced. For n_c this correction is negligible with respect to the other theoretical uncertainties. The correction factor for the semileptonic branching ratio is estimated in [5] to be 0.98 ± 0.03.

In a recent review the value of $n_c = 1.10 \pm 0.06$ was evaluated [6] as the average of the $\Upsilon(4S)$ results; this measurement is driven by CLEO results.

At LEP, OPAL [7] has measured D^0, D^+, D_s^+ and Λ_c^+ production in $Z \to c\bar{c}$ and $Z \to b\bar{b}$ separately, using a two-dimensional fit to the decay length and the fractional energy of the charmed hadrons. DELPHI [8] has also measured D^0 and D^+ production in $Z \to c\bar{c}$ and $Z \to b\bar{b}$ events.

In this work a pure b hemisphere sample is selected by the algorithm developed for the $R_b = \Gamma(Z \to b\bar{b})/\Gamma(Z \to q\bar{q})$ measurement [9]. Charmed hadron candidates are reconstructed in the hemisphere opposite to the b-tagged one, in order to avoid biases on the charmed hadron composition. The high purity of the selected hemispheres makes the measurement nearly insensitive to the systematics coming from the uncertainty of the b selection efficiency.

All weakly decaying charmed hadrons, except for the Ξ_c (the Ξ_c symbol represents both Ξ_c^+ and Ξ_c^0) and the Ω_c, are identified through the exclusive decay channels listed in Table 1, together with the branching ratios used in this paper [10]. The inclusive measurement of n_c is then given by

$$n_c = f(b \to D^0 X) + f(b \to D^+ X) + f(b \to D_s^+ X) + f(b \to \Lambda_c^+ X) + f(b \to \Xi_c X)$$

$$+ f(b \to \Omega_c X) + 2 \times f(b \to \text{charmonia} X)$$

where $f(b \to X_c X)$ is the production rate of the charmed hadron X_c or $\overline{X}_c$ from b.

Char. part.	Final state	BR %	Efficiency %	$c\bar{c}$ %	$g \to c\bar{c}$ %
D^0	$K^-\pi^+$	3.83 ± 0.12	63.7 ± 0.5	0.7	1.6
D^+	$K^-\pi^+\pi^+$	9.1 ± 0.6	31.9 ± 0.4	0.5	1.5
D_s^+	$\phi\pi^+ \to K^-K^+\pi^+$	1.77 ± 0.44	29.8 ± 1.0	0.3	0.7
Λ_c^+	$pK^-\pi^+$	4.4 ± 0.6	22.5 ± 0.9	0.3	0.3

Table 1: Selected final states for the n_c measurement together with their branching ratios, selection efficiency and contaminations from $c\bar{c}$ and $g \to c\bar{c}$ events (given in percent). The efficiency refers to selected b hemispheres. The $c\bar{c}$ contamination is taken from Monte Carlo while the $g \to c\bar{c}$ contribution is normalized to the ALEPH measurement.

2 The ALEPH detector

The ALEPH detector is described in detail in [11] as well as its performance in [12]. A brief review is given in the following.

Charged particles are tracked in an axial magnetic field of 1.5 T using a silicon vertex detector (VDET) with two-dimensional readout, a drift chamber (ITC) and a time projection chamber (TPC). The TPC provides up to 338 measurements of the specific ionization, dE/dx, for each track. In this paper the dE/dx information is considered available when more than 50 measurements are associated to a charged particle.

A normalized particle identification estimator based on the dE/dx measurement is defined as

$$R_P = \frac{(\mathrm{dE/dx})_{\mathrm{measured}} - (\mathrm{dE/dx})_{\mathrm{expected,P}}}{\sigma_{\mathrm{expected,P}}},$$

where $P = p, K, \pi, \ldots$ indicates the particle hypothesis. The dE/dx measurement gives, in the relativistic rise region, a $\pi - K$ separation corresponding to two standard deviations.

The vertex detector has a spatial resolution of 12 μm in $r\phi$ and between 12 and 22 μm for the z coordinate, depending on the polar angle of the track. The inner and the outer layers cover 85% and 69% of the solid angle. The impact parameter resolution can be parametrized, for a track having hits in both VDET layers, as

$$\sigma(\delta) = 25\mu m + \frac{95\mu m}{p(\mathrm{GeV}/c)}.$$

For high momentum particles the transverse momentum resolution is given by

$$\frac{\Delta p_T}{p_T} = 6 \times 10^{-4} \, p_T \, (\mathrm{GeV}/c).$$

Surrounding the tracking detectors are the electromagnetic calorimeter (ECAL), the superconducting solenoid, the hadron calorimeter (HCAL) and the muon chambers. The electromagnetic calorimeter (ECAL) is a lead wire chamber calorimeter with cathode pad readout. The hadron calorimeter (HCAL) is composed by 1.2 m of iron,

2

interleaved with 23 layers of streamer tubes, while the muon chambers consist of two double layers of streamer tubes. The calorimeter readout is organized in projective towers.

3   Event selection and Monte Carlo sample

The measurement is performed on the data sample collected by ALEPH in the period 1992-95. The $Z \to q\bar{q}$ events are selected on the basis of the visible charged energy and multiplicity [13]. It is required that at least five charged particle tracks are detected with a total momentum greater than 10% of the centre-of-mass energy. With these criteria about 3.7 million events are selected.

A high b purity sample is obtained by using the same b tag algorithm exploited in the R_b measurement [9]. The algorithm is based on a combination of a lifetime tag [14] and a mass tag which relies on the large invariant mass of the beauty hadron decays with respect to the charm ones. To avoid any bias of the charmed sample, the b tag is applied to the hemisphere opposite to the charmed hadron candidate.

Events are only considered if the thrust polar angle satisfies the condition $|\cos(\theta)| <$ 0.7 to guarantee a homogeneous VDET acceptance. With this cut a sample of about 230,000 hemispheres is selected. Inside the angular acceptance the b purity of the selected sample is about 99% with an efficiency of the order of 20%, the main source of contamination, according to the Monte Carlo, being $c\bar{c}$ events.

The number of selected b hemispheres is corrected for the c contamination and for the hard gluon emission. A very energetic gluon can bring both b's in the same hemisphere while the gluon can hadronize into light quarks in the opposite, tagged one. This hard gluon emission is estimated, from Monte Carlo, to happen in about 2% of the b events.

In order to compute efficiencies in the various decay channels a Monte Carlo program based on JETSET 7.3 [15] is used. The full detector simulation is applied to the Monte Carlo events which are processed through the same reconstruction program used for real events. The JETSET procedures used for parton shower and string fragmentation are tuned to fit event shape variables [16] and to take into account initial and final state radiation. Heavy flavors events are generated according to the Peterson et al. [17] fragmentation function. The b hadron properties are modified to reproduce the most up-to-date experimental results [18].

A sample of about 5 million $Z \to q\bar{q}$ and 600,000 $Z \to b\bar{b}$ events is used. In addition a dedicated production of a few thousand events is made to reduce the Monte Carlo statistical uncertainty on the efficiency of the $D_s^+ \to \phi\pi$ channel.

4   Charmed particle selection

The charmed particles are identified, in the selected hemispheres, through the exclusive decay channels described in Table 1. The contamination from $Z \to c\bar{c}$ events is evaluated from Monte Carlo, while for the process $g \to c\bar{c}$ the ALEPH measurement [19] $\bar{n}_{g\to c\bar{c}} = (2.65 \pm 0.90)\%$ is used.

3

The efficiencies for reconstructing the charmed hadrons in b selected events are reported in Table 1 together with the $c\bar{c}$ and $g \to c\bar{c}$ contaminations.

4.1 $D^0 \to K^-\pi^+$ selection

Pairs of tracks which form a $K^-\pi^+$ invariant mass in the range $1.7 - 2.1$ GeV/c^2 are considered as D^0 candidates. The kaon candidate must satisfy $R_K < 2$, if the dE/dx information is available. In addition the angle θ^* between the K momentum evaluated in the $K\pi$ rest frame and the $K\pi$ boost direction must satisfy $|\cos(\theta^*)| < 0.8$. The fractional energy $X_E = E(D^0)/E_{\text{beam}}$ of the reconstructed D^0 is required to be greater than 0.15.

4.2 $D^+ \to K^-\pi^+\pi^+$ selection

The $D^+ \to K^-\pi^+\pi^+$ decays do not suffer from the ambiguity of the $D^0 \to K^-\pi^+$ in selecting the kaon track, since the kaon is always the track with opposite sign with respect to the pair of pions. Triplets of tracks with invariant mass in a $1.7 - 2.1$ GeV/c^2 window and with total charge of ± 1 are pre-selected. The X_E of the D^+ candidate is required to be greater than 0.15.

In order to reduce the combinatorial background a cut $|\cos(\theta^*)| < 0.8$ is applied, where θ^* is the angle between the sphericity axis of the three tracks and the D^+ boost direction evaluated in the D^+ rest frame. The dE/dx cut [20] $(R_K + R_\pi) < 1$ is applied to the kaon candidate when available.

The three tracks are required to form a common vertex with a probability greater than 1% and a projected decay length significance along the D^+ momentum greater than 3; the significance is defined as the ratio of the distance of the D^+ vertex from the interaction point, projected along its momentum, over its uncertainty.

In order to reject both fully and partially reconstructed $D^{*+} \to D^0\pi^+$, $D^0 \to K^-\pi^+X$ decays it is required that the invariant mass of each $(K^-\pi^+)\pi^+$ combination satisfies $m(K\pi\pi) - m(K\pi) > 0.15$ GeV/c^2.

4.3 $D_s^+ \to \phi\pi^+$ selection

The D_s^+ candidates are reconstructed in the $D_s^+ \to \phi\pi^+$ decay mode with $\phi \to K^-K^+$. Opposite-sign track pairs with individual momenta greater than 1 GeV/c, a total momentum of at least 2.5 GeV/c and an invariant mass within 8 MeV/c^2 of the ϕ mass [10] are selected as ϕ candidates. The dE/dx of the two kaon candidates must satisfy the requirement $|R_K| < |R_\pi|$, when available. To reconstruct the D_s^+, in addition to the two kaons, the presence of a third track forming a vertex with a probability greater than 1% is required.

The cut $|\cos(\lambda^*)| > 0.4$ is applied, where λ^* is the angle between the kaon direction in the the ϕ rest frame and the ϕ boost direction in the D_s^+ rest frame; this cut relies on the P-wave nature of the decays $D_s^+ \to \phi\pi^+$ and $\phi \to K^+K^-$. The other angular cut applied is $|\cos(\theta^*)| < 0.8$, where θ^* is the angle between the pion and the D_s^+ boost direction evaluated in the D_s^+ rest frame.

4.4 The $\Lambda_c^+ \to pK^-\pi^+$ selection

The selection of the Λ_c^+ candidates relies on the use of the dE/dx measurement. The proton, the kaon and the pion candidates are tracks with a momentum greater than 4.0, 2.0 and 0.5 GeV/c respectively and at least one associated point in VDET. The probability that the three tracks have a common vertex must be greater than 1%.

All three particles are required to have a dE/dx measurement compatible within 2.5σ with the value expected for the corresponding particle hypothesis, when available; the dE/dx measurement is mandatory for kaon and proton candidates. A dE/dx pion veto $|R_\pi| > 2$ is applied to the proton candidate and $|R_\pi| > 1$ to the kaon. For the Λ_c^+ candidate $X_E > 0.2$ is required.

5 Inclusive fraction measurement

In each channel the selected sample contains both signal and background events. The size of the signal is extracted by means of a fit to the mass spectra. The D^0, D^+, D_s^+ and Λ_c^+ mass spectra for the data sample, with the fitted functions superimposed, are shown in Figs. 1 a, b, c, and d respectively.

Monte Carlo studies are performed in order to obtain the appropriate parametrization of the fitting functions for the different mass spectra. To parametrize the D^0 signal two Gaussian distributions plus a flat tail are used; the tail is introduced to take into account badly reconstructed D^0's, which amount to a few percent of the total signal. For the D^+ the vertex requirement strongly reduces the tails so that two Gaussian distributions are sufficient. In the D^0 fit the width of the narrow Gaussian is left free. For the D_s^+ and the Λ_c^+, a single Gaussian with free width is enough to obtain a good parametrization of the signal.

The background can be divided into two categories: the resonant background, coming from partially or wrongly reconstructed decays of charmed hadrons, and the combinatorial background, coming from randomly associated tracks.

In each channel possible resonant contributions, which can distort the signal mass spectrum, are identified and taken into account in the fit. In the D^0 fit, separate functions are used to describe the $D^0 \to K^+\pi^-$ contribution (where the kaon identification is incorrect), the $D^0 \to K^-\pi^+(\pi^0)$ and the $D^0 \to K^-K^+$ channels and the combinatorial background in which one of the two tracks comes from a true D^0 decay. This semi-combinatorial background has a shape which is slightly different from the pure combinatorial. In the D^+ fit the main resonant background arises from the $D_s^+ \to K^+K^-\pi^+$ decays where the K^+ is identified as a π^+; this gives a resonant contribution under the D^+ peak.

In the D^0 fit the pure combinatorial background is parametrized with a third order polynomial, with parameters fitted to the Monte Carlo distributions except for the overall normalization which is left free. In the D^+, D_s^+ and Λ_c^+ fits the background is parametrized as a second order polynomial with free coefficients.

In order to extract the charm production rates in b events, the fit results are corrected for the contamination coming from the $c\bar{c}$ events and from the gluon splitting process $g \to c\bar{c}$ described in section 4. The number of candidates fitted, after the

background subtraction, together with the measured production rates are reported in Table 2. The branching ratios listed in Table 1 are used to determine $f(b \to X_c X)$. The errors are statistical only.

Charmed hadron	N. candidates	$f(b \to X_c X) \cdot BR\%$	$f(b \to X_c X)\%$
$D^0 \to K^- \pi^+$	3318 ± 134	2.32 ± 0.09	60.5 ± 2.4
$D^+ \to K^- \pi^- \pi^+$	1533 ± 86	2.13 ± 0.12	23.4 ± 1.3
$D_s^+ \to \phi \pi^+$ with $\phi \to K^- K^+$	219 ± 23	0.32 ± 0.03	18.3 ± 1.9
$\Lambda_c^+ \to p K^- \pi^+$	251 ± 33	0.48 ± 0.06	11.0 ± 1.4

Table 2: Production rates for the different charmed hadrons obtained from the fit results. The last column is obtained using the branching ratios listed in Table 1.

6 Systematic errors

Since the signal is normalized to the number of selected b hemispheres, the measurement is not affected by errors coming from the $Z \to b\bar{b}$ selection efficiency and, due to the high b purity, the measurement is almost unaffected by the uncertainty on the $c\bar{c}$ contamination.

In the following the different sources of systematic uncertainty are discussed starting with those related to the simulation of the physics properties in the selected Monte Carlo events; in the second part those related to the simulation of the detector performance are evaluated. Each component of the systematic uncertainty is described below and given in Table 3.

Source	$D^0 \to K^- \pi^+$	$D^+ \to K^- \pi^+ \pi^+$	$D_s^+ \to \phi \pi^+$	$\Lambda_c^+ \to p K^- \pi^+$
c contamination	0.7	0.7	0.6	0.6
$\bar{n}_{g \to c\bar{c}}$	0.5	0.3	0.2	0.2
hard gluon emission	0.3	0.3	0.3	0.3
b physics	1.2	1.1	0.9	2.1
Track quality	0.5	0.7	0.7	0.7
dE/dx	0.7	0.6	1.2	1.8
Vertex	-	3.0	2.5	2.5
Signal fitting funcs	1.5	1.6	-	-
Backg. fitting funcs	1.2	1.4	1.0	0.5
MC statistics	0.7	1.2	3.3	4.1
Total systematics	2.7	4.2	4.6	5.7
Branching ratio	3.1	6.6	24.9	13.6

Table 3: Relative systematic errors in percent of the $f(b \to X_c X)$ measurement, for the different channels. The last row contains the relative error coming from the uncertainty on the final state branching ratio.

The charm contamination enters both in the correction to the number of selected hemispheres and in the correction to the number of reconstructed charmed hadrons. To be conservative an independent 50% error on both corrections is applied. According to [19] a 31% uncertainty is applied on the number of charmed hadrons coming from the process $g \to c\bar{c}$. A 30% relative error is assumed on the hard gluon emission correction. The systematics related to the simulation of the b fragmentation and physics properties in the Monte Carlo are evaluated by varying, within errors, the Peterson fragmentation parameter ϵ_b, the topological branching ratios of b hadrons and the fraction of excited b mesons produced in the b fragmentation.

A fraction of the tracks coming from the decay of a charmed hadron can be lost because of nuclear interactions with the detector material or tracking reconstruction errors. The fraction of decays lost due to these effects is evaluated from Monte Carlo to be from 5 to 7% depending on the final state multiplicity. On this quantity a systematic error of 10% is applied.

The performance of the ionization measurement is checked directly on data. The fraction of tracks having the dE/dx measurements available is compared in real and simulated $q\bar{q}$ events. Possible differences in the dE/dx calibration and resolution between Monte Carlo and data are tested with a sample of minimum ionizing pions in $q\bar{q}$ events and a sample of muons in $Z \to \mu^+\mu^-$ events. The differences found between data and Monte Carlo are used to estimate the systematic error on the dE/dx cut. The Λ_c^+ selection has the greatest dependence on the ionization loss measurement; the dE/dx is studied using samples of protons from Λ decays, kaons from D^{+*} decays and pions from K_S^0 decays. The R_p, R_K, and R_π distributions for real protons, kaons and pions respectively show no significant difference between data and Monte Carlo. For the pion veto, small differences in the calibration curves lead to visible effects in the R_π distribution of protons and kaons. This affects mainly the protons which have a $(6 \pm 1)\%$ higher probability in data to survive the pion veto. A correction is applied to the selection efficiency. The efficiency of the kaon selection is verified to within $\pm 1\%$ with this sample. From these studies a systematic uncertainty of 1% on the dE/dx efficiency for kaons and protons is estimated.

The systematic uncertainty associated with the vertex requirement is obtained by studying the fraction of selected track triplets which form a vertex under the mass peak corrected for the background fraction evaluated from the sidebands. The D^+ error also contains the uncertainty due to the decay length cut.

For the D^0 and the D^+, the dependence of the measured yield on the signal fit parameters, which are fixed to the Monte Carlo value, is estimated by repeating the fit with a variation of 5% on these parameters. In the D_s^+ and Λ_c^+ fits all the signal parameters are left free. The coefficients of the combinatorial background are fixed only in the D^0 fit. The dependence on the choice of the parametrization is checked by choosing different fitting functions (second- or third-order polynomial, decreasing exponential). As a second test the background, parametrized as a decreasing exponential, has been left free in normalization and shape in the D^0 fit.

7 The determination of n_c

Measurement	Stat. uncert. .	Sys. uncert.	BR uncert
$f(b \rightarrow D^0 X) = 0.605$	0.024	0.016	0.019
$f(b \rightarrow D^+ X) = 0.234$	0.013	0.010	0.015
$f(b \rightarrow D_s^+ X) = 0.183$	0.019	0.009	0.045
$f(b \rightarrow \Lambda_c^+ X) = 0.110$	0.014	0.006	0.015
$f(b \rightarrow \Xi_c X) = 0.063$	-	0.021	-
$f(b \rightarrow c-\text{onia} X) = 0.017(\times 2)$	0.005	0.011	-
$n_c = 1.230$	0.036	0.038	0.053

Table 4: Different contributions to the n_c determination. In the total systematic error on n_c the correlations between some uncertainties are taken into account.

To measure the average number of charm quarks per b decay all the weakly decaying open charm states must be counted together with charmonia $c\bar{c}$ states, which have to be counted twice.

The total charmonia production rate can be determined from the inclusive ALEPH measurement [21], corrected for the prompt $Z \rightarrow J/\psi$ production estimated by [22], $f(b \rightarrow J/\psi X) = (1.13 \pm 0.16)\%$. The inclusive J/ψ production can be related to the direct one by subtracting the contribution coming from radiative charmonia decays ($\chi_c \rightarrow J/\psi\gamma$, $\psi' \rightarrow J/\psi\gamma$, etc.). This is determined from [23] to be (0.32 ± 0.04). With this correction the direct $f(b \rightarrow J/\psi X) = (0.81 \pm 0.11)\%$ is obtained, where the error includes only the statistical uncertainty coming from the ALEPH measurement.

From this rate, the total charmonia production is determined using the theoretical prediction described in [24]. In that paper the ratio of the direct production rates of the different charmonia states are calculated to be $\eta_c : J/\psi : \chi_{c1} : \psi' = 0.57 : 1 : 0.27 : 0.31$. With this method $f(b \rightarrow \text{charmonia } X) = (1.74 \pm 0.25 \pm 0.57)\%$ is obtained, where a 30% uncertainty on the theoretical prediction of [24] is added to the systematic error.

The charmed strange baryon (Ξ_c, Ω_c) production must be added to complete the charm counting measurement. The b hadron composition at LEP is estimated in [10] to be $(37.8 \pm 2.2)\%$ for each of B^0 and B^+ mesons, $(11.2 \pm 1.9)\%$ for B_s mesons and $(13.2 \pm 4.1)\%$ for b baryons. In the B meson decays the Ξ_c production rate has been measured at CLEO [6] to be $f(B \rightarrow \Xi_c X) = (3.9 \pm 1.5)\%$. The contribution from b baryons has never been measured. The rate $f(b_{\text{baryon}} \rightarrow \Xi_c X)$ is taken from JETSET to be 22% with a 50% relative systematic uncertainty. The rate $f(b_{\text{baryon}} \rightarrow \Omega_c X)$ is assumed to be negligible. Adding together the B meson and b baryon contributions, the charmed strange baryon production rate is estimated to be $f(b \rightarrow \Xi_c X) = (6.3 \pm 2.1)\%$.

The different contributions to n_c measured by ALEPH are listed in Table 4 together with the estimated charmonia and charmed strange baryon production rates. From the sum of these contributions the value of $n_c = 1.230 \pm 0.036_{\text{stat}} \pm 0.038_{\text{sys}} \pm 0.053_{\text{BR}}$ is obtained.

In Fig. 2 the n_c value determined in this paper, together with the most recent ALEPH measurement of the b semileptonic branching ratio [25] (the one obtained

with the charge correlation method), are compared with the theoretical expectation evaluated in [4], showing good agreement.

8   Conclusions

The production rates of the weakly decaying charmed particles D^0, D^+, D_s^+ and Λ_c^+ in $Z \to b\bar{b}$ events have been measured.

A comparison of the inclusive charm production in b decays measured in this and other experiments is shown in Table 5. The average of the $\Upsilon(4S)$ results is taken from a recent review [6].

Experiment	$f(b \to D^0 X)$	$f(b \to D^+ X)$	$f(b \to D_s^+ X)$	$f(b \to \Lambda_c^+ X)$
ALEPH	$60.5 \pm 2.4 \pm 1.6$	$23.4 \pm 1.3 \pm 1.0$	$18.3 \pm 1.9 \pm 0.9$	$11.0 \pm 1.4 \pm 0.6$
DELPHI[8]	$59.4 \pm 3.7 \pm 2.9$	$22.2 \pm 1.9 \pm 1.4$	-	-
OPAL[7]	$53.5 \pm 2.7 \pm 3.1$	$18.8 \pm 1.5 \pm 1.3$	$20.8 \pm 2.2 \pm 2.1$	$12.5 \pm 2.4 \pm 1.0$
$\Upsilon(4S)$[6]	$62.1 \pm 2.0 \pm 3.2$	$24.2 \pm 3.1 \pm 1.6$	$9.8 \pm 0.6 \pm 2.4$	$4.7 \pm 0.7 \pm 1.4$

Table 5: Comparison between the charm production rates (given in percent) in b events for different experiments. The first error is statistical and the second is systematics. The uncertainty on the final state branching ratios is not included. All the LEP results assume the same PDG values of these branching ratios. To extract the DELPHI results the value of $R_b = 0.216$ is used.

The difference with respect to the low energy experiments can be attributed to the different b hadron composition since the presence of B_s and Λ_b at LEP increases the D_s^+ and Λ_c^+ production rates.

From the ALEPH measurements and estimates of the charmonia and charmed strange baryon production rates, the value of the average number of charm quarks per b decay is determined to be

$$n_c = 1.230 \pm 0.036_{\text{stat}} \pm 0.038_{\text{sys}} \pm 0.053_{\text{BR}}.$$

The measured n_c value together with the ALEPH measurement of the b semi-leptonic branching ratio are in good agreement with the theoretical expectation.

Acknowledgments

References

[1] G. Altarelli and S. Petrarca, Phys. Lett. B261 (1991) 303.

[2] I. Bigi et al., Phys. Lett. B323 (1994) 408.

[3] E. Bagan et al., Phys. Lett. B342 (1995) 362;
Phys. Lett. B374 (1996) 363, *erratum* to Phys. Lett. B342 (1995) 362;
Phys. Lett. B351 (1995) 546.

[4] M. Neubert and C.T. Sachrajda, CERN-TH/96-19.

[5] M. Neubert, CERN-TH/96-55.

[6] T. Browder and K. Honscheid, Prog. in Part. and Nucl. Phys. 35 (1995) 81.

[7] The OPAL collaboration, G Alexander et al., CERN-PPE/96-51 (submitted to Z. Phys.).

[8] The DELPHI collaboration, P. Abreu et al., Z. Phys. C59 (1993) 533;
The DELPHI collaboration, *Study of Charm Meson Production in Z Decays and Measurement of* $\Gamma_{charm}/\Gamma_{had}$, Contribution to the EPS-HEP 95 conference, Brussels, EPS0557.

[9] The ALEPH collaboration, *Measurement of* R_b *using a lifetime/mass tag*, PA10-014, contribution to ICHEP96 Warsaw, 25-31 July 1996.

[10] Particle Data Group, R.M. Barnett et al., Phys. Rev. D54(1996) 1.

[11] The ALEPH collaboration, D. Decamp et al., Nucl. Instr. and Meth. A294(1990) 121.

[12] The ALEPH collaboration, D. Buskulic et al., Nucl. Instr. and Meth. A360(1995) 481.

[13] The ALEPH collaboration, D. Decamp et al., Z. Phys. C53 (1992) 1.

[14] The ALEPH collaboration, D. Buskulic et al., Phys. Lett. B 313 (1993) 535.

[15] T. Sjöstrand, Comp. Phys. Comm. 39 (1986) 347;
M. Bengtsson and T. Sjöstrand, Comp. Phys. Comm. 43 (1987) 367.

[16] The ALEPH collaboration, D. Buskulic et al., Z. Phys. C55 (1992) 209.

[17] C. Peterson, D. Schlatter, I. Schmitt and P.M. Zerwas, Phys. Rev. D27 (1983) 105.

[18] The LEP experiments, *Combining Heavy Flavor Electroweak Measurements at LEP*, CERN-PPE/96-017 (submitted to Nucl. Instr. and Meth.).

[19] The ALEPH collaboration, *Measurement of $g \to c\bar{c}$ using D^* mesons*, PA05-065, Contribution to ICHEP96 Warsaw, 25-31 July 1996.

[20] The ALEPH collaboration, D. Buskulic et al., Phys. Lett. B 322 (1994) 275.

[21] The ALEPH collaboration, D. Buskulic et al., Phys. Lett. B295 (1992) 396.

[22] Peter Cho, Phys. Lett. B368 (1996) 171.

[23] The CLEO collaboration, R. Balest et al., Phys. Rev. D52 (1995) 2661.

[24] J.H. Kühn, S. Nussinov and R. Rückl, Z. Phys. C5 (1980) 117.

[25] The ALEPH collaboration, *Measurement of the semileptonic b branching ratios from inclusive leptons in Z decays*, EPS0404, contribution to EPS-HEP Brussells, 27 Jul-2Aug 1995.
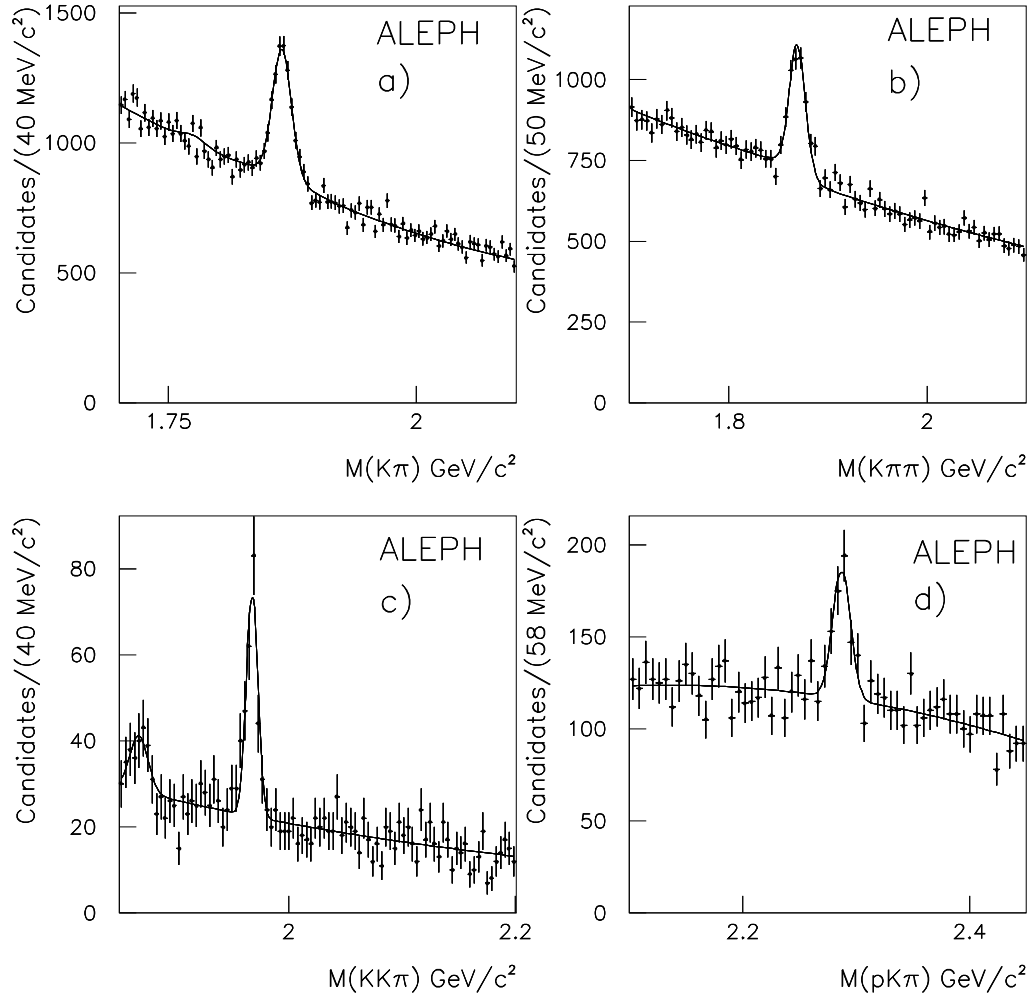
Figure 1: Mass spectrum of the $D^0 \rightarrow K^- \pi^+$ (a), $D^+ \rightarrow K^- \pi^+ \pi^+$ (b), $D_s^+ \rightarrow K^- K^+ \pi^+$ (c) and $\Lambda_c^+ \rightarrow p K^- \pi^+$ (d) candidates, with superimposed the fit result.
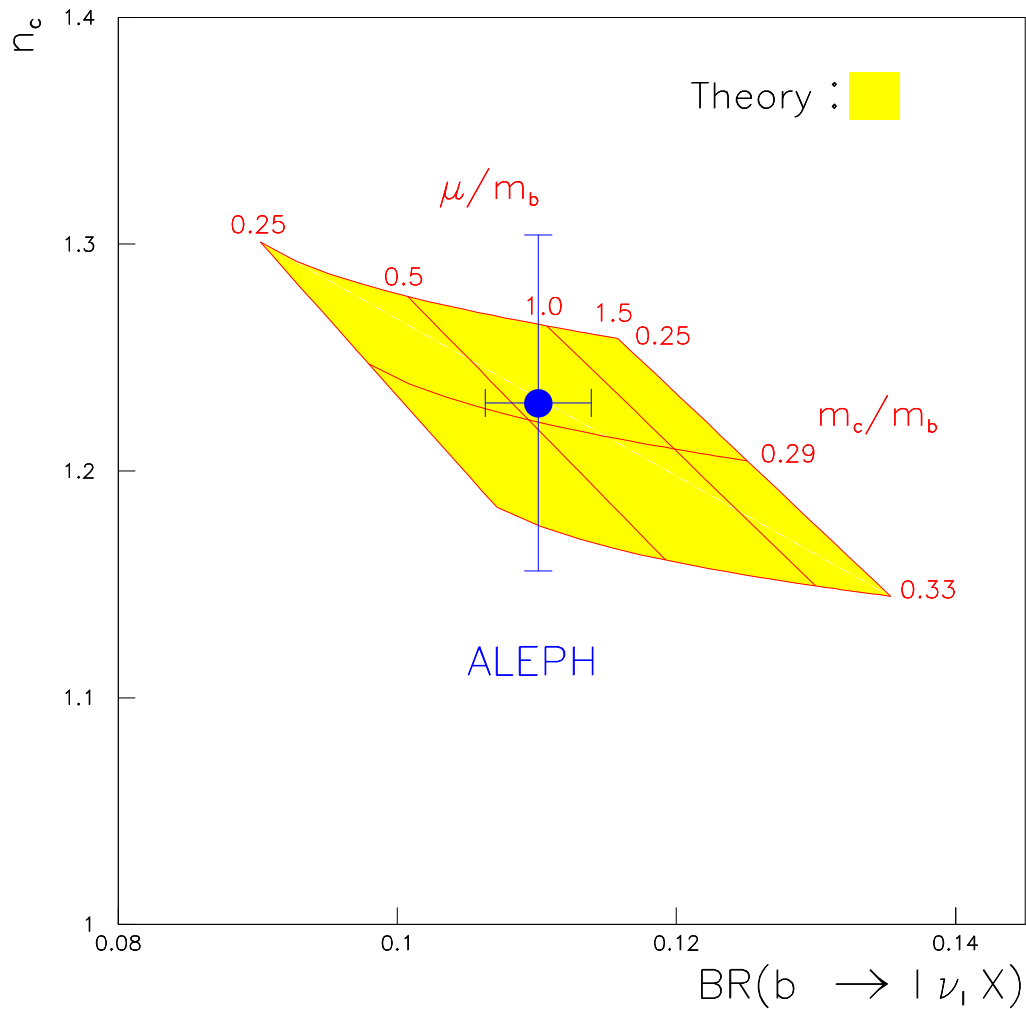
Figure 2: Comparison of the theoretical allowed region [4] in the plane n_c vs $BR(b \to \nu\ell X)$ with the ALEPH measurements. The area represent the region predicted by theory in the on-shell renormalization scheme. The area is obtained by varying the quark masses ratio m_c/m_b in the range 0.25-0.33 and the renormalization scale μ in the range $0.25 < \mu/m_b < 1.5$.